

Designing Hybrid Neural Network Using Physical Neurons - A Case Study of Drill Bit-Rock Interaction Modeling

Zihang Zhang, Xingyong Song

Department of Engineering Technology & Industrial Distribution

Department of Mechanical Engineering

Texas A&M University

College Station, TX 77843

Email: zzhangau@tamu.edu, songxy@tamu.edu

Abstract—Neural networks have been widely applied in system dynamics modeling. One particular type of networks, hybrid neural networks, combine a neural network model with a physical model which can increase rate of convergence in training. However, most existing hybrid neural network methods require an explicit physical model constructed, which sometimes might not be feasible in practice or could weaken the capability of capturing complex and hidden physical phenomena. In this paper, we propose a novel approach to construct a hybrid neural network. The new method incorporates the physical information to the structure of network construction, but does not need an explicit physical model constructed. The method is then applied to modeling of bit-rock interaction in the down-hole drilling system as a case study, to demonstrate its effectiveness in modeling complex process and efficiency of convergence in training.

Index Terms—Neural Network; Bit-Rock Interaction

I. INTRODUCTION

In recent years, neural network (NN) has increasingly been used to model complicated physical system. Unlike the pure physics-based models, NN is a data-based method where the intrinsic physical characteristics within the data are learned by layers of neurons and their connections. Its capability of modeling complex systems and identifying their hidden dynamical features makes the method widely applied in various fields such as agriculture, medical science, engineering and management [1].

The idea of combining the physics-based approach and the neural networks approach together for modeling leads to an emerging category of methods called hybrid neural networks (HNN). By leveraging the known physics information, the training of neural networks can be more efficient with faster convergence. There are primarily two groups of hybrid neural networks. The first group [2], [3] directly adds a neural network model on top of a physical model, where the neural network model is trained using the error between the physical model and the data used for training. The second group [4]–[10] is still primarily based on a physics model, where

some parameters which are hard to observe or compute are trained and obtained using neural networks. However, most existing hybrid networks methods require a physical model to be explicitly constructed. This can cause two issues. First, in many cases, due to the complex physical process behind, constructing an explicit physical model may not be feasible, while only certain physical characteristics can be extracted. Second, directly using a physical model can make the hybrid model more dependent on the physical model and induce bias towards the pre-constructed physical model. If the physical model is not accurately constructed, it can negatively affect the capability of neural networks to capture the actual physical process behind.

In this paper, we intend to explore a new direction of constructing hybrid neural networks. Instead of requiring a physical model to be available, we only assume some physical feature of the system can be reliably captured. We then interpret this physical information into specific neurons and incorporate them in the overall neural network structure. The new method can strengthen the traditional neural networks with physical information, but avoids explicit construction of a physical model.

The new hybrid modeling method will be explained in the context of drill bit-rock interaction modeling as a case study. Down-hole drilling is a critical technology which has been used not only in oil and gas production, but also in enhanced geothermal energy systems (EGS) and specimen extraction in outer space exploration. To analyze, optimize and control the drilling process, it is important to have an accurate and reliable drilling dynamics model. One particular part that is challenging to model is interaction between the drill bit and rock. There are some existing studies to model the bit-rock interaction physically [11]–[16]. However, due to variations in rock/earth property, complex down-hole conditions, it is hard to ensure an accurate and reliable modeling results in practical operating conditions. Therefore, in this paper, we will model the bit-rock interaction using a new hybrid neural network framework to demonstrate its effectiveness.

The rest of the paper is organized as the following. Firstly, the physical process of the bit-rock interaction is explained in section II. Secondly, section III discusses the method to build the HNN structure. Then section IV explains how the training data is obtained using a laboratory scale setup. Finally, the training results are presented in section V. The model is compared with the traditional neural network and pure physical model on test data. It is concluded the proposed method has better performance in terms of convergence and accuracy.

II. PHYSICS OF BIT-ROCK INTERACTION

According to [15], the drilling dynamics can be essentially described by a low dimension model. Based on the modeling method described in [17], the drilling system is simulated as a low-dimensional lumped-parameter model. As shown in Figure 1, the drilling system is divided into two portions with top drive and drill string as the top portion and the bottom hole assembly (BHA) with the drill bit as the bottom portion.

Since the drill string dynamics is known and well-established, this research will focus on modeling the bit-rock interaction, including weight and torque on bit denoted as W_b and T_b , which are typically hard to model due to the complex downhole condition and rock cutting process. The method in [14] [17] is chosen as the baseline physical bit-rock interaction model. Note that, the baseline physical model referred here is only used for benchmark purpose in the result analysis and is not required in the construction of the hybrid neural network model. The description of the physical model below also explains some well known physics of the bit-rock interaction that will be incorporated into the hybrid model construction in the next section. Nevertheless, only part of the physics, rather than the full physical model, will be used in the hybrid model. The magnitudes of the force and torque components are determined by a physical variable called depth-of-cut. Depth-of-cut is defined as the total contact depth of the drill bit with the rock-cutting surface, which is governed by

$$d(t) = n(x_1(t) - x_1(t - \tau(t))) \quad (1)$$

where n is the number of the blades, x_1 is the axial displacement of the drill bit, and $\tau(t)$ represents the delay for the blade to rotate the angle difference between two successive blades, described as

$$\frac{2\pi}{n} = \theta_1(t) - \theta_1(t - \tau(t)) \quad (2)$$

where θ_1 is the angular displacement of the drill bit.

When $d < 0$, the drill bit is not in contact with the rock thus the reaction force and torque are both zero. Consider $d \geq 0$, the contact force and torque are separated into frictional and cutting components, denoted as

$$W_b(t) = W_b^f(t) + W_b^c(t) \quad (3)$$

$$T_b(t) = T_b^f(t) + T_b^c(t) \quad (4)$$

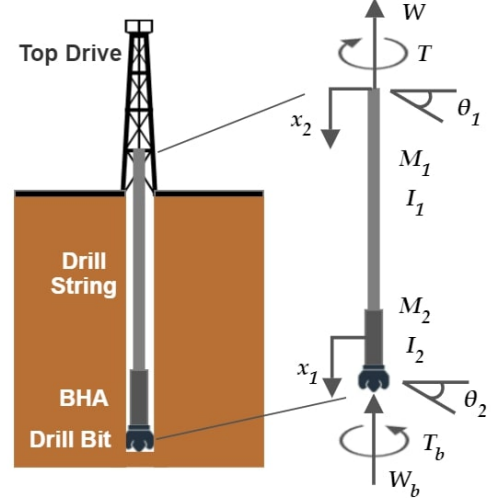


Fig. 1 Drill string schematic

The cutting component is contributed by the removal of the rock in the cutting process, which is expressed as

$$W_b^c(t) = a\zeta\epsilon d(t) \quad (5)$$

$$T_b^c(t) = \frac{1}{2}a^2\epsilon d(t) \quad (6)$$

where a denotes the radius of the drill bit, ζ is a characteristic coefficient of the cutting surface orientation, ϵ is the intrinsic specific energy to destroy a unit volume of rock.

The frictional component will first increase as the depth-of-cut increases, and become saturated when the depth-of-cut reaches a threshold value. Let d^* be the threshold value, then the frictional component is given as

$$W_b^f(t) = \begin{cases} W_{b1}^f(t) = a\sigma\kappa d(t)^{\frac{1+\text{sign}(\dot{x}_1)}{2}} & d < d^* \\ W_{b2}^f(t) = a\sigma\kappa d^* & d \geq d^* \end{cases} \quad (7)$$

$$T_b^f(t) = \frac{1}{2}a\mu\gamma W_b^f(t) \quad (8)$$

where σ denotes the maximum normal stress, κ represents the rate of variance of the contact length, μ is the coefficient of friction, γ is a characteristic parameter representing the orientation and distribution of the contact forces.

In order to have a smooth derivative, a smooth transition is used between the two phases at d^* , the frictional force components is rewritten as

$$W_b^f(t) = W_{b1}^f(t) \frac{1 - \tanh \lambda(d(t) - d^* + \delta)}{2} + W_{b2}^f(t) \frac{1 + \tanh \lambda(d(t) - d^* - \delta)}{2} \quad (9)$$

where λ and δ are smoothing factors.

III. NEURAL NETWORK STRUCTURE

The limitation of the physical model above is that it can only be used to describe the process in an ideal condition. However, there can be other physical processes such as the flush of drilling fluid and possible accumulation of

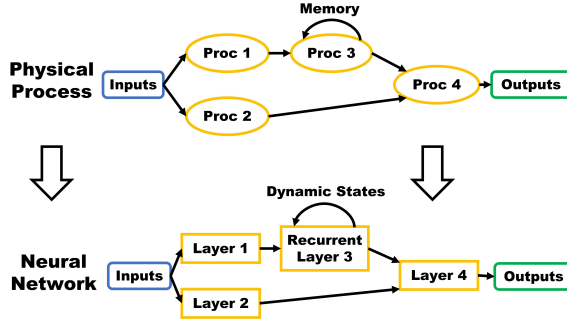


Fig. 2 Interpreting Physics to network structure

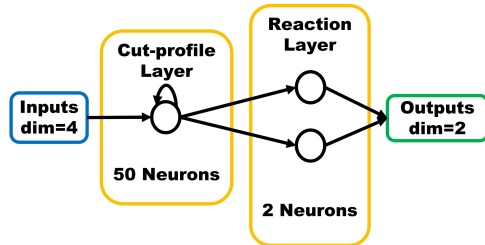


Fig. 3 Layers of the proposed hybrid neural network

drilling rocks close to the bit that can impact the bit rock interaction but are hard to be explicitly modeled. To address this limitation, we propose to use a hybrid neural network model (HNN) to model the bit-rock interaction process. The HNN does not need to rely on the physical model explained in Section II, but only incorporates some well-known physics in bit-rock interaction such as the depth of cut.

A. Incorporating Physics to Network Layers

As implied in Figure 2, the physical process of bit-rock interaction is firstly decomposed to several processes, each of the process is defined as a layer of the network and outputs some physical parameters or states. If a process involves memories of states, it is interpreted as a recurrent layer. Otherwise a general fully connected layer is applied.

Based on this method, the network structure to model the bit-rock interaction is shown in Figure 3: It has two layers, the first layer is the recurrent layer which takes drill bit states as inputs and outputs a cut profile which is the height of the rock relative to the drill bit, at sampled angles between two successive blades. The second layer outputs the reaction force and torque based on depth-of-cut information from the first layer output. Denote the inputs of the layers as \mathbf{y}_1 , \mathbf{y}_2 and the outputs of the layers as \mathbf{z}_1 , \mathbf{z}_2 . The input to the network \mathbf{y}_1 consists of the axial displacement and velocity, torsional displacement and velocity. The details of each layer are shown below.

1) **Cut Profile Layer:** This layer is a recurrent layer since the cut profile, which is the trajectory of the blade in $\frac{2\pi}{n}$ rad range, is a dynamic memory required to derive the next cut profile. The forward method of this layer at time t is written

as

$$\mathbf{z}_1^{t+1} = F_1(\mathbf{y}_1^t, \mathbf{z}_1^t) \quad (10)$$

In the following section the function F_1 is derived based on the interpolation formula.

Firstly, a general interpolation formula is defined as follows: Write $\mathbf{a} = [a_1, a_2, \dots, a_i]$, $\mathbf{b} = [b_1, b_2, \dots, b_i]$, assume $a_1 < a_2 < a_3 < \dots < a_i$, define the interpolated trajectory of points (a_1, b_1) , (a_2, b_2) , \dots , (a_i, b_i) as

$$I(x; \mathbf{a}, \mathbf{b}) : [a_1, a_i] \rightarrow \mathbb{R} \quad (11)$$

For simplicity, we use linear interpolation in this case study, which is

$$I(x; \mathbf{a}, \mathbf{b}) = b_j + \frac{(x-a_j)(b_{j+1}-b_j)}{a_{j+1}-a_j}, \quad a_j \leq x < a_{j+1} \quad (12)$$

Secondly, the sampled points are computed. Assume there are p hidden layers (p outputs) in this layer, then at time t , they are written as $\mathbf{z}_1^t = [z_1^t, z_2^t, \dots, z_p^t]^T$, and each hidden state represents the heights of rock relative to the drill bit at sampled angles, i.e. $\phi_1 = \frac{2\pi}{n} \frac{1}{p}$, $\phi_2 = \frac{2\pi}{n} \frac{2}{p}$, \dots , $\phi_{p-1} = \frac{2\pi}{n} \frac{p-1}{p}$, $\phi_p = \frac{2\pi}{n}$ in rad. Let $\hat{\phi} = [\phi_1, \phi_2, \dots, \phi_p]^T$, the sampled points are denoted as $(0, 0)$, (ϕ_1, z_1^t) , (ϕ_2, z_2^t) , \dots , (ϕ_p, z_p^t) . The sampled points coordinates are denoted as $\hat{\phi} = [0, \phi_1, \phi_2, \dots, \phi_p]$ and $\hat{\mathbf{z}} = [0, z_1^t, z_2^t, \dots, z_p^t]$.

Thirdly, the new sample points are computed when the layer receives a new input. The inputs can be decomposed to the axial and the torsional displacements of the drill bit, denoted as $\delta x_1^t, \delta \theta_1^t$, by which the sampling points are shifted. The new sampling points coordinates after the displacement are derived as

$$\hat{\phi} = [0, \delta \theta_1^t, \phi_1 + \delta \theta_1^t, \phi_2 + \delta \theta_1^t, \dots, \phi_p + \delta \theta_1^t] \quad (13)$$

$$\hat{\mathbf{z}} = [0, \delta x_1^t, z_1^t + \delta x_1^t, z_2^t + \delta x_1^t, \dots, z_p^t + \delta x_1^t] \quad (14)$$

Finally, the outputs are derived based on the interpolated trajectory of the new points, which is $I(\theta; \hat{\phi}, \hat{\mathbf{z}})$, thus the forward method can be derived as

$$\mathbf{z}_1^{t+1} = F_1(\mathbf{y}_1^t, \mathbf{z}_1^t) = I(\phi; \hat{\phi}, \hat{\mathbf{z}}) \quad (15)$$

which is to apply the interpolation at sampled angles ϕ to the sampling points $(\hat{\phi}_i, \hat{z}_i)$.

2) **Reaction Layer:** This layer outputs the weight-on-bit and torque on bit based on the cut profile from the last layer. According to the definitions, depth-of-cut is equal to the axial displacement of drill bit within $\frac{2\pi}{n}$ torsional displacement, that is $d = y_{2,p}$, where $y_{2,i}$ denotes the i th element of \mathbf{y}_2 . Based on the equations 3 to 9, when drill bit velocities are positive, the reaction force and torque can be denoted as a function of depth-of-cut $W_b(d; \Theta)$, $T_b(d; \Theta)$ where Θ is the set of physical parameters in bit-rock interaction, the forward method is written as

$$\mathbf{z}_2 = \begin{bmatrix} W_b(\mathbf{y}_{2,p}; \Theta) \\ T_b(\mathbf{y}_{2,p}; \Theta) \end{bmatrix} + W_R \mathbf{y} + b_R \quad (16)$$

where W_R and b are weights and bias respectively.

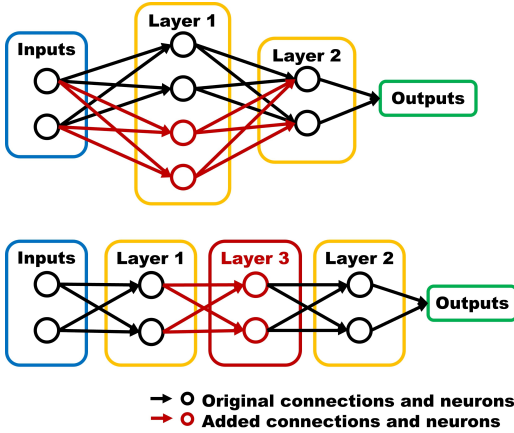


Fig. 4 Ways to add structures to increase network complexity. Top: additional neurons; Bottom: additional layers

In this layer, Θ , W_R and b are the learnable parameters. Based on the physics of bit-rock interaction described in Section II, Θ can be described by four independent parameters which are $[a\zeta\epsilon \quad \frac{1}{2}a^2\epsilon \quad a\sigma\kappa \quad \frac{1}{2}a^2\mu\gamma\sigma\kappa]$. W_R and b are both initialized as zeros to keep the physical information.

Note that the equations 3 to 9 provide an initial guess of the structure and parameters but the network does not rely on that. The physical parameters are assumed to be inaccurate and are learned during training. Even without a physical model, this layer can be replaced with a general function approximator. Nevertheless, the embedded known information will help improve the convergence and accuracy.

Finally a RELU activation function is added to this layer since the negative depth-of-cut implements no contact between the bit and the rock and zero reaction force or torque.

B. Increasing the Network Complexity

The neural network with only physical information incorporated is not sufficient to address any hidden dynamics or uncertainties within the physical process. Therefore, it is necessary to increase the network complexity to improve its capability of modeling complex process. This can be achieved by adding additional neurons and connections as well as additional layers.

1) Additional Neurons and Connections: As depicted at the top figure of 4, additional neurons and connections can be added to an existing layer. The weights of the additional connections to the former layer are initialized to zeros, making the initial values of the new neurons be zero, and the weights to the next layer are randomly initialized. This maintains the original physical properties of the neuron network and at the same time add network complexity to address uncertainties.

In the proposed network new connections are added in cut-profile layer, which originally is a recurrent layer without learnable parameters. The neurons are now connected the same way as Gated Recurrent Unit (GRU), with TANH activation function. GRU connections include an update and a reset gate [18], which are used to process the memory of the layer.

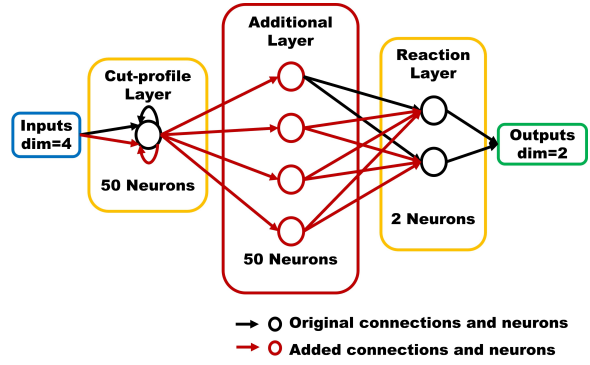


Fig. 5 Final structure of the proposed hybrid neural network

2) Additional Layers: The bottom figure in Figure 4 shows another way to improve complexity which is to add additional fully connected layer (Layer 3) between existing layers (Layers 1 and 2) in series. The initial weights and bias of the new layer are designed to maintain the physical information in the original network, so that the outputs of Layer 1 in the original network (Figure 4) are also included in the outputs of the new layer added. This helps keep the physical information transmitted between Layer 1 and Layer 2 in the original network, and at the same time any unmodeled process or dynamics between Layers 1 and 2 can be captured by the new layer (Layer 3 in Figure 4).

Specifically, in our proposed network, a new layer with 50 neurons is added between the cut-profile layer and the reaction layer, shown in Figure 5. It has two learnable parameters: weights $W \in \mathbb{R}^{50 \times 50}$ and bias $B \in \mathbb{R}^{50 \times 1}$.

To maintain the physical information transferred from the cut profile layer to the reaction layer, the first rows of W and B are initialized as $W_1 = [0 \ 0 \ 0 \ \dots \ 0 \ 1]$, $B_1 = 0$. Other rows of W and B are randomly initialized.

The final network structure for bit-rock interaction model is shown in Figure 5. It consists of 3 layers: the recurrent cut-profile layer has 50 hidden units/outputs. The depth-of-cut layer is a fully connected layer with 50 outputs. The reaction layer outputs axial and torsional control inputs.

IV. TRAINING AND TESTING DATA

Typically, it is hard to access field testing data for down-hole drilling system, and real-time force/torque data close to the drill bit is even more rare. Therefore, a lab scale down-hole drilling rig was built in the lab and testing data was obtained to validate the proposed model.

Given the limited load that can be exerted on the lab scale system, the final data used is a combination of data from a physical model and data collected from experiment. The data collected from the physical model is used to as a baseline, and the data from experiment is to replicate uncertainty such as the effect of accumulation of rocks, etc. The dimension of the data is 4×10000 , with sampling frequency of $200Hz$, and time ranging from 0 to 50 seconds. The first 10 seconds are used for training while the next 40 seconds are used for testing. The data for training is shown in Figure 6.

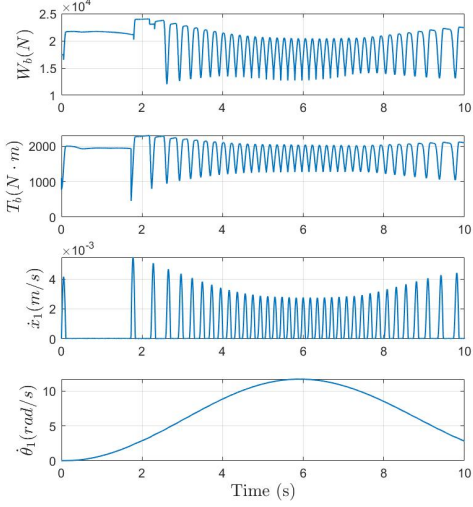


Fig. 6 Data used for training, from top to bottom: force, torque, axial velocity, torsional velocity

TABLE I Parameters of drilling model

M_1	44187 kg	I_1	1685 kgm^2
M_2	29028 kg	I_2	1187 kgm^2
C_a	34400 Ns/m	C_t	49.5 Nms/rad
K_a	353000 N/m	K_t	495 Nm/ra
ϵ	77e6 Pa	$\gamma\mu$	0.7
ζ	0.64	n	5
κ	5	σ	6.2572e7 Pa
a	0.15 m	d^*	1.8721e-4 m
λ	5e4	δ	6e-07

TABLE II RMSE of different methods on testing data

Method	Reaction Force	Reaction Torque
Hybrid Network	1007.4	75.8
Traditional Network	3401.7	355.5
Physical Model	2736.5	452.4

V. RESULTS

The hybrid neural network, as explained in section III, is trained on the data obtained in section IV. In comparison, the same data is used to train a traditional neural network. This network has 4 layers: the first layer is a recurrent GRU layer with 50 neurons and TANH activation function, followed by 2 fully connected layers each with 50 neurons and RELU activation function, and a fully connected layer with 2 outputs at last. In addition, the initial conditions of the hybrid network are shifted by random constants. The physical parameters used of the drilling system is shown in table I. The learning rates of both networks are set to 0.005.

A. Training

The training progress is shown in Figure 7 and the results are shown in Figures 8 and 9. According to Figure 7, the loss of the traditional network decreases but the rate of change gets smaller after 5 episodes, and the loss remains almost

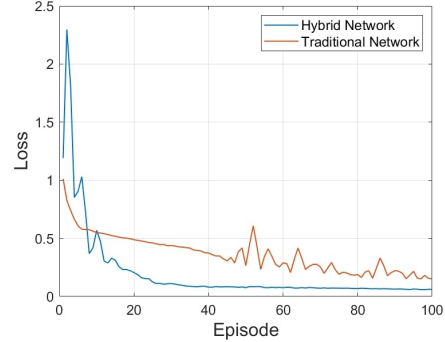


Fig. 7 Training progress of different Neural Networks

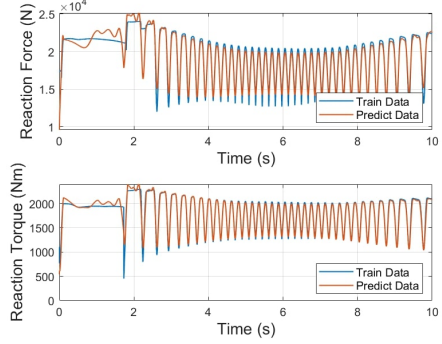


Fig. 8 Training results of Hybrid Neural Network

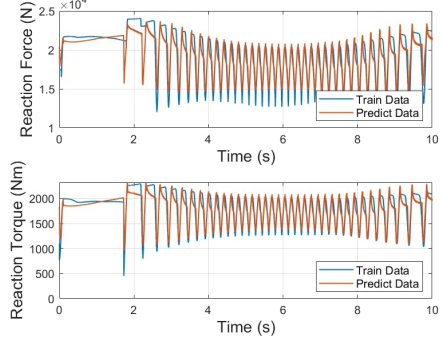


Fig. 9 Training results of traditional Neural Network

the same after 70 episodes, implying the convergence of the neural network. The final loss is around 0.16.

For the hybrid neural network, it has higher initial loss than the traditional network. The loss increases at first but quickly drops as the training processes. It converges to around 0.15 and does not change too much after 40 episodes. This implies the hybrid network has a much faster convergence rate.

B. Testing

Both models are applied to testing data for validation, and the results are shown in Figures 10 and 11. It is observed that the hybrid network model has smaller magnitude error, implementing that the hybrid network is more suitable to predict data in the long-term future.

In addition, the modeling result is also compared to using a pure physical model described in Section II. It can be shown

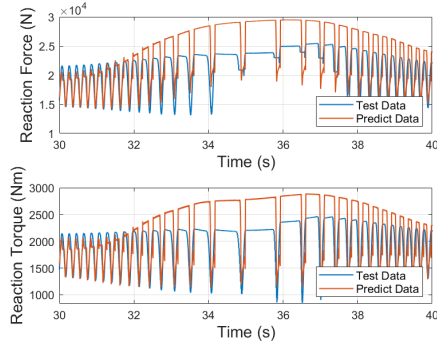


Fig. 10 Test results of traditional Neural Network

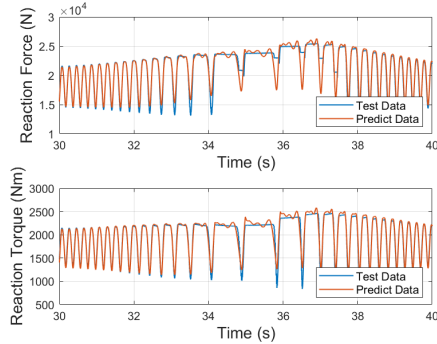


Fig. 11 Test results of Hybrid Neural Network

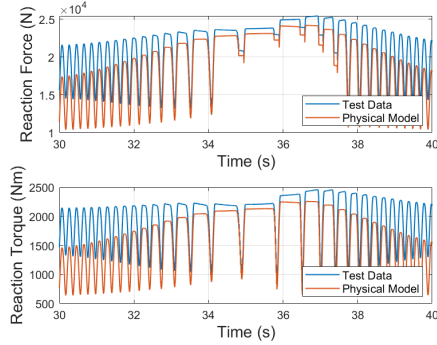


Fig. 12 Simulation results of physical model

in Figure 12 that the accuracy of the proposed approach is also higher than that using physical model only.

A summary of root mean squared error (RMSE) is shown in Table II to quantify the performance of different methods.

VI. CONCLUSION

A new method is presented to build a hybrid network by interpreting the physical information into specific neurons and incorporating them in the overall neural network structure. The new hybrid method does not require a physical model to be explicitly available. We then use modeling of bit-rock interaction in the down-hole drilling process as a case study. The training results, as compared with the results from a traditional neural network and a benchmark physical model,

show that the hybrid network is more effective in terms of convergence rate and modeling accuracy.

REFERENCES

- [1] O. I. Abiodun, A. Jantan, A. E. Omolara, K. V. Dada, N. A. Mohamed, and H. Arshad, "State-of-the-art in artificial neural network applications: A survey," *Helijon*, vol. 4, no. 11, p. e00938, 2018.
- [2] H. E. Garcia and R. B. Vilim, "Combining physical modeling, neural processing, and likelihood testing for online process monitoring," in *SMC'98 Conference Proceedings. 1998 IEEE International Conference on Systems, Man, and Cybernetics (Cat. No. 98CH36218)*, vol. 1. IEEE, 1998, pp. 806–810.
- [3] U. Forssell and P. Lindsjog, "Combining semi-physical and neural network modeling: An example of its usefulness," *IFAC Proceedings Volumes*, vol. 30, no. 11, pp. 767–770, 1997.
- [4] E. Piron, E. Latrille, and F. Rene, "Application of artificial neural networks for crossflow microfiltration modelling: 'black-box' and semi-physical approaches," *Computers & chemical engineering*, vol. 21, no. 9, pp. 1021–1030, 1997.
- [5] H. Qi, X.-G. Zhou, L.-H. Liu, and W.-K. Yuan, "A hybrid neural network-first principles model for fixed-bed reactor," *Chemical Engineering Science*, vol. 54, no. 13–14, pp. 2521–2526, 1999.
- [6] S. Wang, F. Wang, V. K. Devabhaktuni, and Q.-J. Zhang, "A hybrid neural and circuit-based model structure for microwave modeling," in *1999 29th European Microwave Conference*, vol. 1. IEEE, 1999, pp. 174–177.
- [7] A. Dolara, F. Grimaccia, S. Leva, M. Mussetta, and E. Ogliari, "A physical hybrid artificial neural network for short term forecasting of pv plant power output," *Energies*, vol. 8, no. 2, pp. 1138–1153, 2015.
- [8] M. Cao, K. Wang, Y. Fujii, and W. Tobler, "A hybrid neural network approach for the development of friction component dynamic model," *J. Dyn. Sys., Meas., Control*, vol. 126, no. 1, pp. 144–153, 2004.
- [9] J. Roubos, P. Krabben, M. Setnes, R. Babuska, J. Heijnen, and H. Verbruggen, "Hybrid model development for fed-batch bioprocesses; combining physical equations with the metabolic network and black-box kinetics," in *6th Workshop on fuzzy systems, September*. Citeseer, 1999, pp. 8–9.
- [10] P. Olaussen, D. Haugstvedt, J. Arriagada, E. Dahlquist, and M. Assadi, "Hybrid model of an evaporative gas turbine power plant utilizing physical models and artificial neural networks," in *Turbo Expo: Power for Land, Sea, and Air*, vol. 36843, 2003, pp. 299–306.
- [11] A. Balanov, N. Janson, P. V. McClintock, R. Tucker, and C. Wang, "Bifurcation analysis of a neutral delay differential equation modelling the torsional motion of a driven drill-string," *Chaos, Solitons & Fractals*, vol. 15, no. 2, pp. 381–394, 2003.
- [12] Y. Khulief, F. Al-Sulaiman, and S. Bashmal, "Vibration analysis of drillstrings with self-excited stick-slip oscillations," *Journal of Sound and Vibration*, vol. 299, no. 3, pp. 540–558, 2007.
- [13] T. Richard, C. Germay, and E. Detournay, "A simplified model to explore the root cause of stick-slip vibrations in drilling systems with drag bits," *Journal of sound and vibration*, vol. 305, no. 3, pp. 432–456, 2007.
- [14] B. Besselink, T. Vromen, N. Kremers, and N. Van De Wouw, "Analysis and control of stick-slip oscillations in drilling systems," *IEEE transactions on control systems technology*, vol. 24, no. 5, pp. 1582–1593, 2015.
- [15] C. Germay, V. Denoël, and E. Detournay, "Multiple mode analysis of the self-excited vibrations of rotary drilling systems," *Journal of Sound and Vibration*, vol. 325, no. 1–2, pp. 362–381, 2009.
- [16] T. G. Ritto, C. Soize, and R. Sampaio, "Non-linear dynamics of a drillstring with uncertain model of the bit–rock interaction," *International Journal of Non-Linear Mechanics*, vol. 44, no. 8, pp. 865–876, 2009.
- [17] D. Tian and X. Song, "Control of a downhole drilling system using integral barrier lyapunov functionals," in *2019 American Control Conference (ACC)*. IEEE, 2019, pp. 1349–1354.
- [18] K. Cho, B. Van Merriënboer, C. Gulcehre, D. Bahdanau, F. Bougares, H. Schwenk, and Y. Bengio, "Learning phrase representations using rnn encoder-decoder for statistical machine translation," *arXiv preprint arXiv:1406.1078*, 2014.